In-situ experimental investigation on the growth of aerosols along the absorption column in post combustion carbon capture

Harsha, Shreyas; Khakharia, Purvil; Huizinga, Arjen ; Monteiro, Juliana; Goetheer, Earl; Vlugt, Thijs

Citation (APA)
Harsha, S., Khakharia, P., Huizinga, A., Monteiro, J., Goetheer, E., & Vlugt, T. (2019). In-situ experimental investigation on the growth of aerosols along the absorption column in post combustion carbon capture. *International Journal of Greenhouse Gas Control*, *85*, 86-99. https://doi.org/10.1016/j.ijggc.2019.02.012

Important note
To cite this publication, please use the final published version (if applicable).
Please check the document version above.

In-situ experimental investigation on the growth of aerosols along the absorption column in Post Combustion Carbon Capture

Shreyas Harsha[1,2], Purvil Khakharia[1*,], Arjen Huizinga[1], Juliana Monteiro[1], Earl Goetheer[1], Thijs J.H Vlugt[2]

[1]TNO, Sustainable Process and Energy System, Leeghwaterstraat 44, Delft,2628CA, The Netherlands
[2] TU Delft, Process & Energy Department Leeghwaterstraat 39, Delft, 2628CB, The Netherlands
*Corresponding author. Tel.: +31 888664543.
E-mail address: purvil.khakharia@tno.nl

Abstract

The amine-based post combustion carbon capture process is one of the most advanced and preferred technologies to reduce CO_2 emissions from point sources like power plants. The emissions of amine from capture plants is one of the biggest challenges faced by this technology. These emissions typically occur by means of aerosol/mist formation. To develop effective countermeasures, it is crucial to understand the dynamic behavior of aerosols within the column, which is currently not well understood. This manuscript presents the results from a study aiming to understand the mechanism of aerosol growth and its behavior along the absorber column in terms of particles number concentration, particle size distribution, and amine emissions. For that, a series of experiments were performed in TNO's bench scale CO_2 capture plant using 30 wt% monoethnolamine (MEA) as solvent. For a SO_3 and CO_2 concentrations of 5.25ppm and 12.5 vol.% in the flue gas, MEA emissions at the top exit of the column were recorded as 1051mg/Nm^3 (with vapour emissions of 381mg/Nm^3). In the absence of SO_3 in the flue gas, inlet particle concentration was 2.71 x 10^7/cm^3 and resulting MEA emissions reduced by 63.5% to 383mg/Nm^3.

From the bottom of the column until the point of maximum temperature, the MEA content in the vapour phase was consistent with the volatility of the solvent. After this point it drastically increases to 1051 mg/Nm^3. Both the number of particles and the total particle mass has lowered from the bottom to the top of the column. For the benchmark test, inlet and outlet total particle concentration were found to be 6.24x10^7/cm^3 and 2.3x10^7/cm^3 respectively, while total particle mass is 2.22mg/m^3 at inlet and 1.32mg/m^3 at outlet. Particles with a dimeter below 0.006μm contribute the most to total particle concentration both at the inlet (50%) and outlet (32%), while particles with diameter of 0.087μm contributes the most to the total particle mass at inlet (47%) and outlet (55%). The measured total mass of particles was in the order of magnitude of 1mg/m^3. This is much lower than the expected aerosol mass emissions, in the order of magnitude of 1 g/Nm^3 based on FTIR emissions.

No particles larger than 0.147μm were recorded, which might explain the low total mass recorded. The cause for this is still under investigation, but it suggests that the sampling procedure may induce systematic errors to the measurements. Nonetheless, the observations from this study have given further insight into the aerosol dynamics in the absorber column and corresponding emissions.

Keywords: CO2 capture; aerosol growth; ELPI; absorber profile.

1. Introduction

One of the biggest challenges the world faces today is climate change. For many years greenhouse gas (GHG) emissions have been linked to the drastic climate change, with CO_2 causing more than 50% of the GHG radiative forcing [1]. Before the start of the industrial revolution in 19th century, the global average CO_2 in the atmosphere was 280ppm. As of 2015, the CO_2 levels in the atmosphere has crossed 400ppm. The growth of CO_2 in the last two decades is 100-200 times faster than that observed during transition from Ice Age. [2] Even though renewable energy is one of the most promising solutions to reduce further emissions of CO_2 and other greenhouse gases, the ever-rising use of fossil fuels would not help in controlling CO_2 emissions into the atmosphere. With the supply of fossil fuels like coal lasting for at least another 30 years [3], the demand for the fuel would not reduce in these 3 decades and consequently, CO_2 will be emitted into the atmosphere.

Post combustion carbon capture (PCCC) is one of the most advanced and preferred methods to capture CO_2 from large point source like power plants. The most commonly used solvent for the purpose of PCCC is Monoethanolamine - MEA (30wt% aqueous solution). However, the drawbacks of this technology are energy intensity and loss of solvent [4][5][6]. This is because of two major reasons; (i) solvent loss leads to higher operating cost, and (ii) amines react with NO_X present in the atmosphere to form nitrosamine [8] which have been reported to have carcinogenic property [9]. For this technology to be applied on a large scale, it would be vital to have solvent emissions under the design criteria of 12 mg/Nm^3 [7]. Amine emissions from the scrubbing unit of the PCCC occurs in two different ways. Firstly, it occurs in gas phase due to the vapour pressure and are called vapour based solvent emissions. The other means of amine emissions is due to the formation of mist/aerosols. This kind of emission is called aerosol-based emission. The reason for aerosol and mist formation within the absorption column is the presence of aerosol nuclei. Various field studies show that the presence of aerosol nuclei in the flue gas results in the rise of aerosol-based emissions from a PCCC [4][7][10][11].

The use of counter-measures like having a well-designed water wash section in place have been effective in abating vapour-based emission [12]. For aiding the development of a high efficiency counter-measure for aerosol-based amine emission, a concrete understanding of mechanism of aerosol formation and growth is needed. Over the years, various studies both experimentally and by means of modelling have contributed to that understanding [13][14][15]. Majeed et.al [16] have characterized the behaviour of aerosols along the absorber column by means of simulation using MEA as model solvent. It was concluded that aerosols grow as they travel along the column irrespective of their initial size with a maximum of 5.25 times initial size(radius). However, the initial composition of droplets had a significant impact on the amine emission from the absorber. Moreover, an increase in initial particle (aerosol) concentration lead to increase in amine emissions ranging from a maximum MEA emission of 200 mg/Nm^3 at 1000 particles/cm^3 to 45000 mg/Nm^3 at 10^7 particles/cm^3. Majeed et.al [17] modelled the behaviour of a single aerosol inside an absorber column using MEA as model solvent. It was noted that initially the size of aerosol reduces at the lower portion of the absorber. Once it reaches a stable size, the aerosols start increasing in size. Moreover, the initial size of the aerosol has an influence on the extent of growth. It was found that aerosol with 0.15μm grows across the column by 2.05 times to attain a final size of 2.2 μm while aerosol with initial size of 1.5 μm grows by 3 times to 4.5 μm. Initial aerosol composition did not significantly affect the final size of the aerosol and only varied by 10%. However, models and simulation studies conducted by Majeed et.al [16][17] cannot be compared and/or validated to experimental data as not all data are publicly available. Also, the model developed by Majeed et.al[16][17] assume all particles entering the absorber to be of the same size which is not observed in reality. Moreover, the aerosols considered in these studies do not account for sulphuric acid aerosols and does not consider mechanisms like Coalescence and Breakup. Zhang et.al [18] simulated the aerosol growth using Piperazine as model solvent in gPROMS. Growth of aerosols across the column was observed with a much significant growth in the water wash. It was noted that in the presence of extra packing, the residence time increased which resulted in further aerosol growth. Higher temperature inside the column resulted in a fast growth of aerosols.

Field measurements of aerosols have been performed in both lab-scale and real-scale CO_2 capture units in the past [7][15][19][20][21][22][23][24]. Mertens et.al[19] carried out a first of its kind study to measure particle concentration and size distribution of aerosols entering and leaving the absorber in a pilot CO_2 capture plant. It was found that the size of aerosols entering the absorber were very small (<0.1μm) with concentrations exceeding 10^8/cm^3. Upon leaving the absorber, the size of aerosols appears to have increased while remaining <1μm and slightly reducing in concentration thereby indicating possible coagulation inside the column. Similar aerosol measurements were performed by Saha et.al[22] at NCCC. During the study conducted at NCCC, the aerosols were measured around the water wash tower. Particles in the range of 10^6-10^7/cm^3 were observed which coincided with that observed in literature. These real time measurements of aerosols have only been performed downstream or upstream of the absorber column. However, there have not been any realistic size distribution of aerosols inside the column itself making it difficult to understand their behaviour within the column and validate the models.

The aim of this research is to provide first of its kind experimental data to predict the trend of aerosols inside the column. These aerosol trends along the column would be observed in terms of number of particles, particle size distribution and amine content in the vapour and aerosol phases. Similar measurements would be performed in the

absence of aerosol causing nuclei and without the presence of solvent along the column. These studies would help in understanding the effect of SO_2 and solvent (MEA) on particulate matter respectively.

2. Test setup, Equipment and Sampling

2.1. CO$_2$ capture mini-plant

In order to replicate the effects of PCCC, TNO's carbon capture bench scale plant, herein referred to as the mini-plant, was used. The mini-plant is a fully automated absorber desorber system with flue gas capacity of 4m^3/h STP. The absorber is a packed bed column with an internal diameter of 45mm. In total there are 5 packed sections with are well insulated from outside within the column, along with an uninsulated section placed at the top of the absorber column. This uninsulated section acts as a cooler to reduce the vapour-based emissions of solvent. Each packed section consists of Sulzer BX type packing with a diameter of 44.96mm and height of 860mm. All the sections are connected to each other by means of flanges.

Fig.1 represents the schematic positioning of various thermocouples along with the gas sampling positions. In total 18 thermocouples are placed across the column to measure the gas and liquid temperatures. The placement of these thermocouples is such that, each packing section of the absorber has of 3 thermocouples each (top, middle and bottom). Similarly, 3 temperature sensors are also placed in the uninsulated part of the column. For the purpose of gas sampling, there exists sampling ports at the beginning of each section (labelled as Tg in Fig. 1). Liquid sampling ports are also available to enable sampling of solvent. The MEA and CO_2 loading of the solvent was measured by means of an Attenuated Total Reflectance type FTIR.

The stripper column has 4 packed sections, each of 510mm in height and 45mm in diameter. Similar to the absorber, Sulzer BX types of 44.96mm diameter were used. During the course of this study, gases were mixed in appropriate proportions to replicate flue gas from a coal fired power plant.

2.2. Aerosol generator

By using a suitable catalyst (V_2O_5), SO_2 was converted to SO_3 in a fixed bed reactor. A mixture of nitrogen, oxygen and SO_2 enters the reactor, that operates at 400 to 550ºC. This enables the gas to heat up sufficiently inside the reactor for the oxidation of SO_2 to SO_3 to take place. In the catalytic production of SO_3 the reaction first proceeds at high temperature of 440-550 °C. As the reaction nears completion, the temperature reduces to around 400°C [25]. Although passive insulation is provided, the gas stream loses heat to the environment before entering a water quench column at 200°C. Water from a vessel at about 50°C is circulated co-currently with the flue gas at a flow of 8 L/h. The water vapour reacts with SO_3 in the flue gas and forms sulphuric acid aerosols. By using a hydro-cyclone at the bottom of the quench column, water droplets from the flue gas are knocked out. CO_2 and compressed air were added at the quench outlet to make up the CO_2 concentration. The artificial flue gas is connected to the mini-plant by a heated line so that the gas enters the mini-plant at about 40°C.
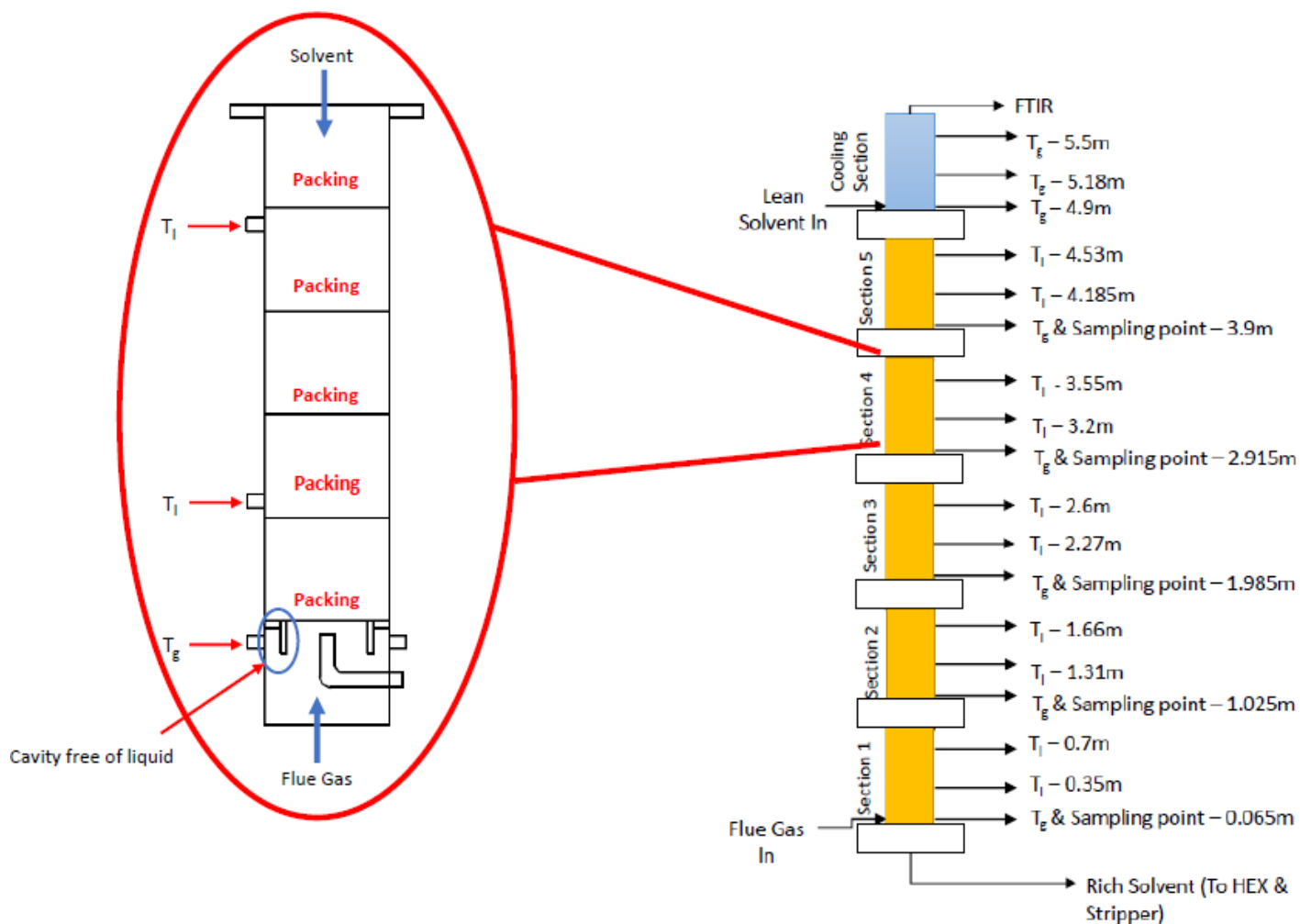
Fig. 1. Schematic representation of positioning of various thermocouples and gas sampling ports with their corresponding heights across the absorber column. T_g refers to gas temperature sensor and T_l refers to the liquid temperature sensor. The figure also illustrates the zoomed in view of a single section. Due to the design of the packing support and distributor in each section, a region that is free of any liquid is present and is used to measure the gas temperature.

2.3. FTIR

Analysis of gas composition is done by means of a Fourier Transform Infrared Spectroscopy (FTIR). (GASMET DX4000), which is calibrated for water vapor (vol. %), CO_2 (vol%), ammonia (vol%), oxygen (vol%) and MEA (mg/Nm^3). Further description and information about the FTIR can be found in literature [26]. To avoid condensation in the sampling line between the FTIR analyzer and sampling probe, the sampling line is heated and maintained at 180°C. Further, the heated probe is also kept at 180°C. The emission values of MEA measured by the FTIR include both vapour based and aerosol-based emissions. Any further mention of MEA emission through FTIR refers to the total MEA content. In order to obtain the emission without the contribution of aerosols, tests without the H$_2$SO$_4$ aerosol nuclei were conducted. The MEA emission recorded in this test are vapour-based emissions (referred to as base case).
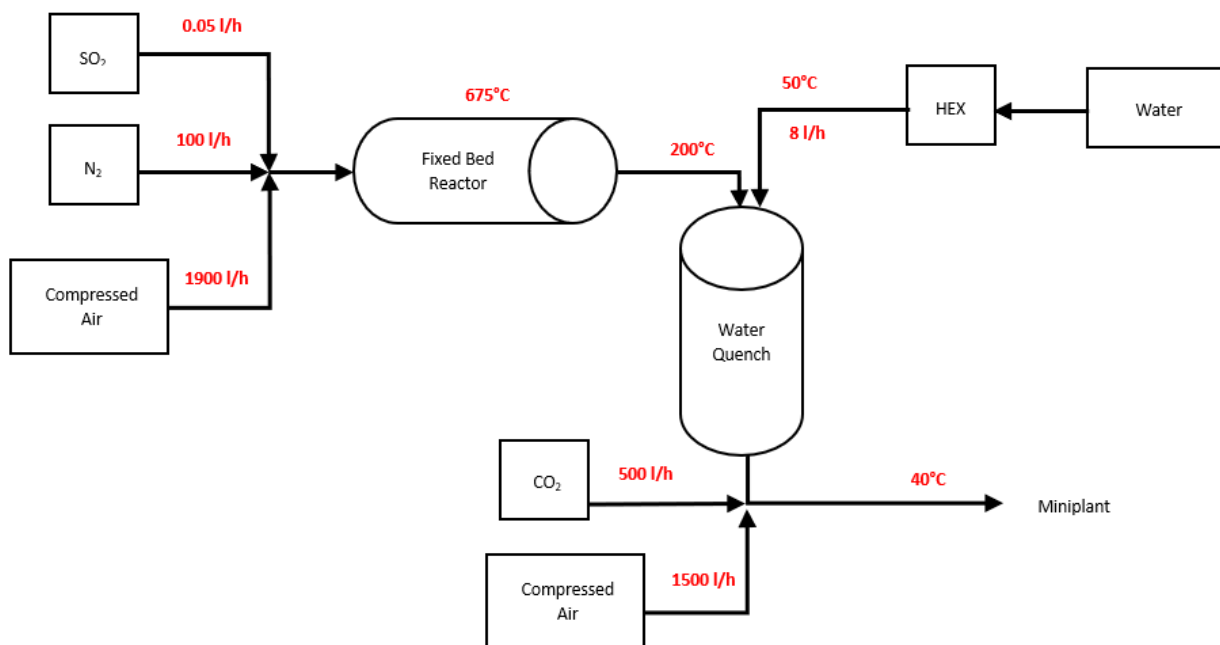
Fig. 2. Schematic representation of flue gas and aerosol generator setup used in this study. The figure also represents the typical temperatures across the setup. Air, N_2, SO_2 are mixed together before passing it through the reactor, which converts SO_2 to SO_3. Gas with converted SO_3 enters a quench column along with water at 50°C to form sulphuric acid nuclei. At the exit of the quench, water is removed by means of a cyclone and recirculated. Gas stream with H_2SO_4 nuclei is mixed with CO_2 and compressed air before entering the absorber.

2.4. ELPI

Electrical Low-Pressure Impactor (ELPI) is a device that enables real time measurements of particles size distribution and its number concentration in a gas stream. The device has the ability of measuring particles in the range of 6nm-10μm. For the purpose of aerosol measurement in this study, Dekati High-Temperature ELPI®+ (HT-ELPI+) was used, which is an advanced version of the normal ELPI®+. Using HT-ELPI+ allows particles measurements at elevated temperature of up to 180°C, which eliminates the possibility of condensation during gas sampling. Detailed explanations of ELPI+ are provided in literature [26][27]. For the durations for this study, impactor was maintained at 80 °C.
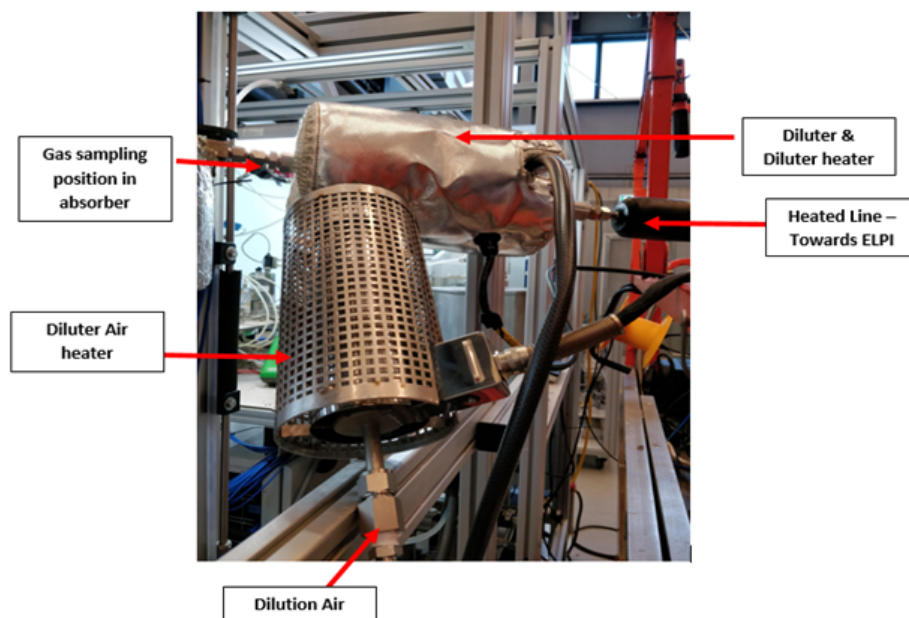

Fig. 3. Gas Sampling setup used for particle measurement.

2.5. Dilution System

During the sampling of the gas, a diluter system was used as the expected total number concentration exceeded 10^7 per cm^3, which is the maximum range of the ELPI$^+$. DEKATI Diluter DI-1000 was used for this purpose. For dilution, N_2 from gas cylinder of 99.5% purity was used. The diluter is based on the concept of ejection dilution, where dilution gas enters through an ejector nozzle. This creates a pressure drop which causes the sample gas (in this case gas from the absorber) to flow through the nozzle. In the mixing chamber, the dilution gas and sample gas mixes well. A part of the gas stream enters the ELPI+ which has a fixed suction flow rate and the remaining gas exits via an exhaust port. This exhaust port was in turn used as a sampling port for the FTIR.

Fig 4 shows a picture of the gas sampling setup. To avoid cooling and in turn condensation of the gas, the dilution gas was heated be means of an air heater. Diluter was also heated to the desired temperature which could be controlled using an external temperature controller. A heated line carries the diluted sample gas to the ELPI$^+$.

Each diluter is individually calibrated for the exact dilution factor by DEKATI for various pressure difference (Inlet pressure – Outlet pressure) and sample gas flow rate. These calibration values are provided in the data sheet by the manufacturer. In this study, the dilution factor was predominantly maintained at 1:8 corresponding to exhaust pressure of 1013 mbar. The velocity of the gas in the absorber stream was 0.69m/s, while the velocity in the dilutor sampling probe was 0.29 m/s.

Gas sampling with ELPI and FTIR were performed across all the sections across the absorber column. This enabled an overview of the gas composition and particle/aerosol number distribution at various positions of the column.
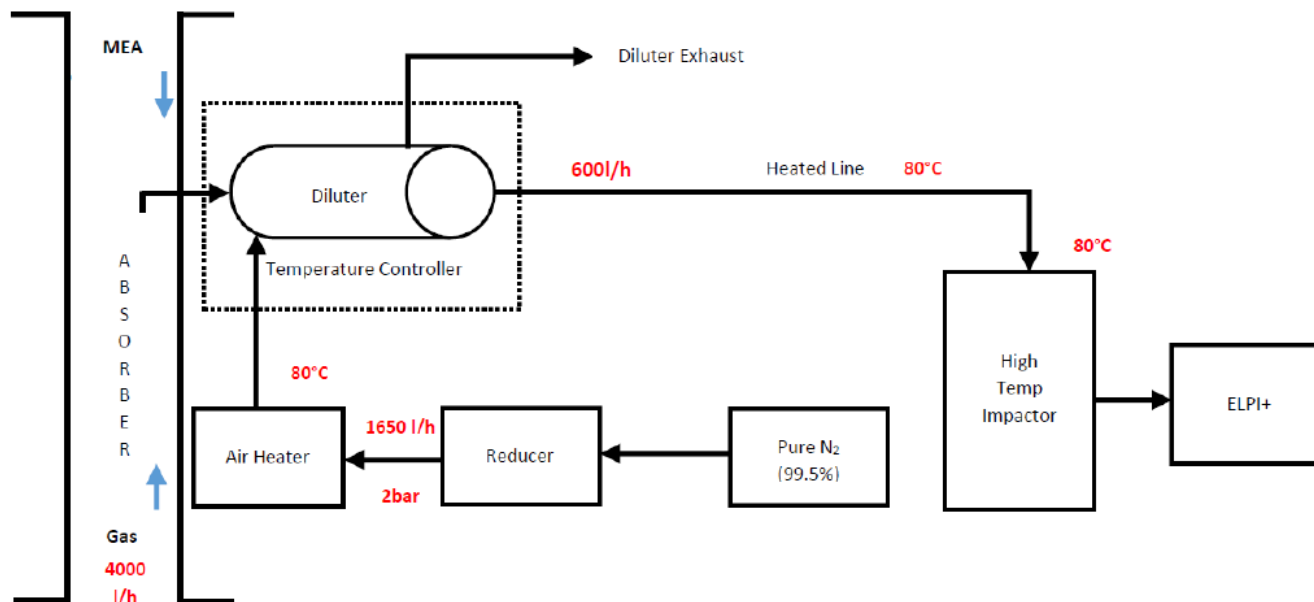

Fig. 4. Schematic representation of the gas sampling technique used for particles measurements using ELPI. 4m^3/h of gas flows through the absorber. A small part of this gas is extracted into the Diluter unit which is maintained at 80°C. To dilute the sampled gas, pure N_2 is used at 2bar. Before entering the diluter and mixing with the sampling gas, the dilution air (N_2) passes through an air heater to heat the gas to 80°C. From the diluter, the diluted sample gas is extracted into the impactor of ELPI at a rate of 600l/h. Excess gas from the diluter exits through the exhaust port.

2.6. Results and Discussion

2.6.1. Column operating parameters

Before any particles measurements or gas analysis were performed, it was made sure that the absorber – desorber unit was stable for at least an hour. Table 1 represents the composition of the flue gas used during this study. Unless otherwise stated, the composition of the flue gas was kept constant. Fig.7 represents the temperature profile within the absorber column. The vertical axis represents the height of the absorber column. Height of 0m represents the gas inlet of the absorber. The temperature increases gradually from bottom to top, with the maximum temperature at a height of ~3.7m. The point of maximum temperature inside the absorber occurs at the top $1/3^{rd}$ part of the column. This observation coincides with the kind temperature profile predicted by models and observed in a typical full-scale absorber. [28][29][30].

Table 1. Composition of Flue Gas used during this study. Compressed air composition is assumed to be 79 vol% N_2 and 21 vol% O_2. (*)Calculated

Gas	Content
N_2	67 vol%
O_2	17.1 vol%
SO_3 (assuming 100% conversion)	5.25ppm
CO_2	12.5 vol%
Water Content*	3.4 vol%

In terms of the solvent composition, CO_2 content in lean solvent was maintained around 1.42 mol/L (±0.12 mol/L) with MEA content of 25.2 wt% (±0.56 wt%). To compare various tests that were performed during this study, the operating conditions mentioned in Table 2 were considered as the benchmark.

Table 2. Operating conditions of the pilot CO2 capture plant. The table provides the averaged value over the period of testing along with the standard deviation when averaged.

Flue Gas Flow [m^3]	Lean Solvent Flow [kg/h]	Inlet solvent temperature (°C)	Inlet gas temperature (°C)	CO_2 content at Inlet (vol %)	Top Stripper Pressure (mbar)	CO_2 content lean solvent (mol CO_2/L solvent)
4	19.98±0.137	41.69±0.07	41.8±0.61	12.48	871±4.01	1.41

2.6.2. Aerosol Mechanism

Various models in literature have described the formation and growth of aerosols as they travel across the absorber column [17][18]. Table 3 presents an overview of the possible routes an aerosol could experience within the absorber column. It also states how these routes influence the particles number and particle mass concentration. Aerosol growth can be attributed to mass transfer from vapor to aerosol (change type 3) and/or agglomeration of particles (change type 2). The former would result in same total number concentration, a size shift to larger size and increase in total mass, while the latter would result in decrease in total number concentration, a size shift to larger size and same total mass.

Aerosol shrinkage can be attributed to mass transfer from aerosol to vapor (change type 4) with resulting decrease in total mass and the same total number concentration. Loss of both particle number concentration and mass concentration can be attributed to aerosols hitting either the solid surfaces present inside the column like or the liquid phase (type 1). Formation of many tiny particles due to the break-up of large particles would result in an increase in total particle concentration but would maintain the same mass. This would be attributed to splitting of particles (type 5). Due to the formation of many tiny particles and decrease in number concentration of larger particles, a shift in particles size distribution towards the left would be observed. Type 5 mechanism has been

reported by Moser et. al in the presence of WESP [23]. In the experiments performed within this work, no external forces are present that could lead to splitting of aerosol particles. Hence, change type 5 is not considered in the analyses.

Table 3. Overview of all the possible routes an aerosol can experience inside of an absorber column. The table represents for each case if there would be an increase/decrease in total number concentration and mass concentration. "Particle Size Distribution shift" represents which side the PSD would shift (Left- increase in small particles; Right - increase in large particles) for each phenomenon, when measured downstream of a section.

Change Type	Phenomena	Total Particle concentration	Total Mass concentration	Particle Size Distribution Shift
1	Hitting on Surfaces (wall and packing)	Reduction	Reduction	No change
2	Agglomeration of smaller aerosols	Reduction	Same	Right
3	Vapour to Aerosol Mass Transfer	Same	Increase	Right
4	Aerosol to Vapour Mass transfer	Same/Reduction	Reduction	Left
5	Splitting of Aerosol	Increase	Same	Left

2.6.3. Empty Column Test

To be able to get a clear picture of aerosol interactions with themselves and the hardware, without the effect of solvent coming into play, an "Empty Column Test" was performed. In this test, gas was passed though the column without any solvent flow into the column. It is important to note that in the absence of solvent phase, following phenomenon do not occur - vapour to aerosol mass transfer and aerosol to vapour mass transfer and a constant temperature profile along the column can be maintained. Particle measurements were performed at every section of the column. Since there was no CO_2 capture, the temperature remains constant inside the column (at ca. 40ºC).

Impactor plates, air heater and diluter system were maintained at 80°C. Similar to the benchmark test, flue gas was passed through the quench system to form H_2SO_4 aerosols. During this test, particles larger than 0.147 μm were not observed like in the benchmark test. Table.4 shows $\Delta N\%$ (ratio of "difference in particle concentration between two consecutive section" to "particle concentration at the lower section") for all the size fractions across the column.

Table 4. Overview of $\Delta N\%$ for empty column test. $\Delta N\%$ is calculated for every size fraction across the column. Positive value of $\Delta N\%$ represents an increase in number of particles.

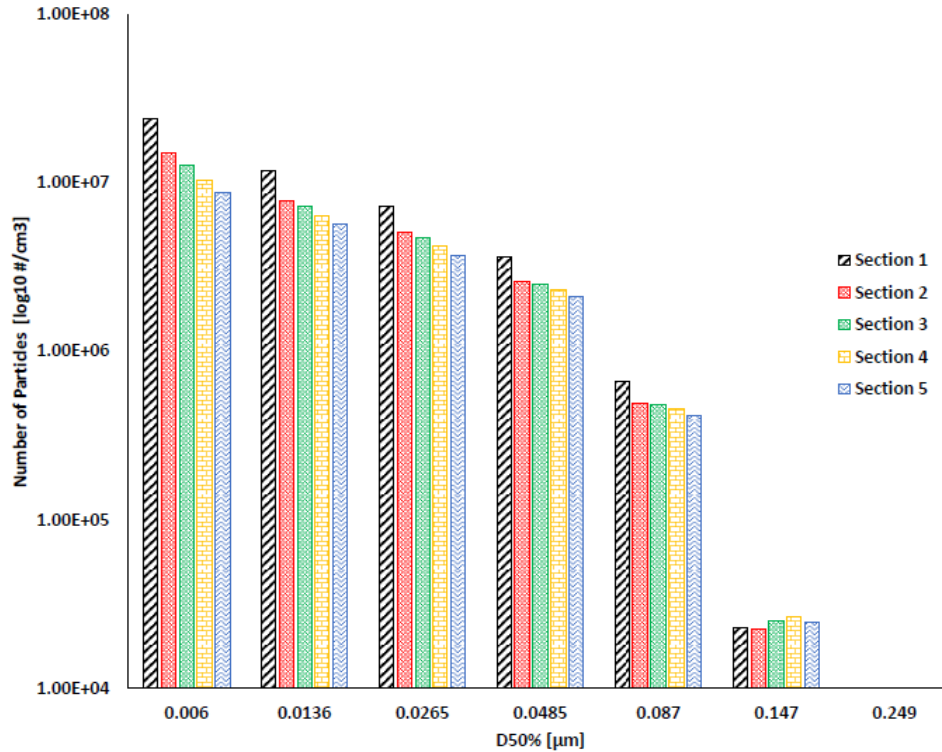| D50%(μm)	0.006	0.0136	0.0265	0.0485	0.087	0.147
$\Delta N_{4-5}\%$	-17%	-12%	-13%	-9%	-9%	-6%
$\Delta N_{3-4}\%$	-18%	-12%	-9%	-7%	-5%	5%
$\Delta N_{2-3}\%$	-16%	-8%	-7%	-4%	-2%	13%
$\Delta N_{1-2}\%$	-37%	-33%	-31%	-28%	-26%	-3%

Fig. 5. Particle Size Distribution for Empty Column Test. During this test, the solvent flow in the column was switched off, thus resulting in zero capture. Like the benchmark test, particles larger than 0.147μm were not observed. Aerosol measurement at each section of the column was performed for a period of 5-6 minutes. Maximum Relative Standard Deviation (RSD) from mean was found to be 10.5%

Fig.5 represents the particle size distribution for the empty column test along the column. It is observed that particles measured range between 0.006-0.147μm in size. Particles larger than 0.147μm were not observed across the whole column. Moreover, the total particle concentration at the inlet was recorded as $4.74 \times 10^7/cm^3$, while at section 5 it reduces by over 50% to $2.06 \times 10^7/cm^3$. Between inlet (section 1) and section 5, the total particle concentration gradually decreases with particles in the range of 0.006-0.147μm. From Table 4 it is observed that for $\Delta N_{1-2}\%$, the loss of particles is relatively high compared to other sections in the column. This trend is as a result of the change in path of flue gas when it enters the column as explained below.

Comparing the $\Delta N_{1-2}\%$ for various size fractions, it is seen that for the largest size fraction of 0.147 μm, the value is relatively low compared to the smaller fractions. Based on the $\Delta N_{1-2}\%$, it is suggested that there occur two phenomena that explains the behavior of aerosols. Firstly, particles between 0.006 μm and 0.087 μm agglomerate leading to form particles of larger diameter, such as 0.147μm. Due to this phenomenon, particles between 0.006 μm and 0.087 μm decrease in number concentration and a negative value for $\Delta N\%$ is observed. The other phenomenon that plays a role is hitting of particles on solid surfaces. At the inlet of the column, due to the bend in tubing, larger particles with heavier mass tend to meet the wall. Consequently, a decrease in number concentration of larger particles is to be observed (negative value of $\Delta N\%$).

Increase in number concentration of larger particles, due to agglomeration of smaller particles along with decrease in number concentration of larger particles due to hitting on solid surfaces, results in a relatively lower value of $\Delta N_{1,2}\%$ for the large particles compared to that for smaller size fraction. Along the column, the probability of hitting solid surfaces reduces (as opposed to at the column entrance) but does not cease to exist.

Table 5 presents the difference in mass of aerosols between two consecutive ($\Delta M_{i,i+1}$) sections along the column. A positive value of $\Delta M_{i,i+1}$ indicates an increase in mass of aerosols in the higher of the two stages. It is observed that the mass gained across section 2&3 ($\Delta M_{2,3}$) for 0.147μm is 4.88E-03 mg/m³ which is less than the total mass lost across section 2&3 ($\Delta M_{2,3}$) in the size range of 0.006μm-0.087μm (1.43E-02 mg/m³). The excess mass lost would be because of hitting on walls. Similar observation can be made between section 3 and 4 of the column.

Table 5. Overview of $\Delta M_{i,i+1}$ (mg/m³) for empty column test. $\Delta M_{i,i+1}$ is the measure of difference of mass between two consecutive sections in the column for various size fraction. A positive value of $\Delta M_{i,i+1}$ indicates increase in mass of aerosols in the higher of the two sections

D50%(μm)	0.006	0.0136	0.0265	0.0485	0.087	0.147
$\Delta M_{4,5}$(mg/m³)	-1.98E-04	-9.83E-04	-5.19E-03	-1.29E-02	-1.42E-02	-2.63E-03
$\Delta M_{3,4}$(mg/m³)	-2.52E-04	-1.12E-03	-4.29E-03	-1.12E-02	-8.88E-03	2.14E-03
$\Delta M_{2,3}$(mg/m³)	-2.77E-04	-7.95E-04	-3.56E-03	-5.74E-03	-3.96E-03	4.88E-03
$\Delta M_{1,2}$(mg/m³)	-1.02E-03	-5.15E-03	-2.21E-02	-6.12E-02	-6.06E-02	-1.02E-03

Brachert et.al [24] have shown by means of simulation and experimental data, the occurrence of agglomeration (referred to as "Coagulation") of sulphuric acid aerosols inside an absorber column. Polydisperse coagulation simulation of aerosols were performed using the data obtained from model developed on AerCoDe. For a sulphuric acid concentration of 5mg/m3 (STP), the arithmetic mean diameter from inlet to exit of column increased from 0.0156μm to 0.021μm. Based on the experiments performed by Brachert et.al [24] a decrease in particle concentration between two measurement point were observed, indicating agglomeration of particles. There were three measurement positions which were separated by 2s and 3.8s from one another. Between these point the total particle concentration reduced by 24.5% and 41.5%, respectively. In this study, the measurement points were separate by 1.4s wherein the total particle concentration reduced between 10-15% (expect between the first two measurement positions). This also indicated the relation between extent of coagulation and residence time inside the column.

2.6.4. Benchmark Test
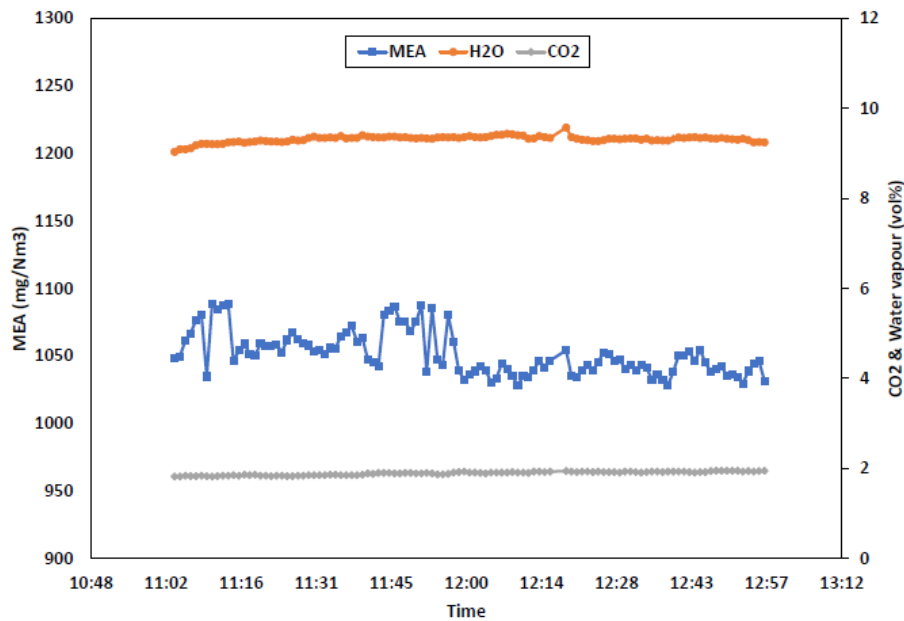
2.6.4.1. Gas composition along the column

Fig. 6. FTIR measurements at the outlet of the absorber column for the benchmark test. The orange line represents the content of water coming out of the column, while the grey line represents the content of CO_2. The measured CO_2 would be measured on wet basis. The blue line represents the amount of ethanolamine exiting the column in mg/Nm³.

Table 6 gives an overview of the results obtained from various measurements and calculations. The CO_2 content measured by a CO_2 analyser is taken for calculation of capture rate.

Fig.6 represents the FTIR measurement at the outlet of the absorber. The water and CO_2 content are constant, while some variation in the MEA, ± 50 mg/Nm^3, is observed. This indicates that the system was stable during the experiment period.

To get an overview of the gas composition along the column, FTIR measurements were made at every section of the column. For this, the exhaust of the diluter was connected to the FTIR. As shown in Fig 8, CO_2 in the gas phase decreases continuously, with the maximum decrease from 1.03 m to 3.9 m. A corresponding increase in water vapour concentration is seen. The MEA content shows a decrease from the inlet to about 2 m into the column. This corresponds also to the temperature rise as a result of released heat of reaction. Although the temperature is increasing along the column, due to the increased loading of the solvent and thus, lower activity of MEA, its emission reduces.

From the maximum temperature (bulge) point to the top of the column, the MEA content increases significantly, from 125 to 1051 mg/Nm^3. The vapour-based MEA emission at the top was found to be 381mg/Nm^3 based on the MEA emissions measured when SO_2 was absent from the flue gas (further explained in section 2.6.5). When aerosol causing nuclei are absent from the flue gas, MEA emissions from the absorber are due to the volatile nature of the solvent and hence can be considered as vapour based emissions. Until the bulge point, the MEA content is in the range of expected volatile emission. However, from the bulge point onwards, the MEA content increases. This shows that when the temperature reduces, the gas phase MEA, instead of condensing back to the bulk solvent phase, is transferred to the aerosol droplets. This results in the significantly higher MEA emission in the gas/aerosol phase. It can be assumed that very little MEA is transferred to the aerosol phase after the lean solvent inlet, and all the transfer occurs from section 5 (i.e. 3.9 m) until lean solvent inlet point at 4.9 m. Unfortunately, there is no gas sampling point available just above the lean solvent inlet. Temperature measurements downstream the lean solvent inlet shows no significant difference, as shown in Fig 7.
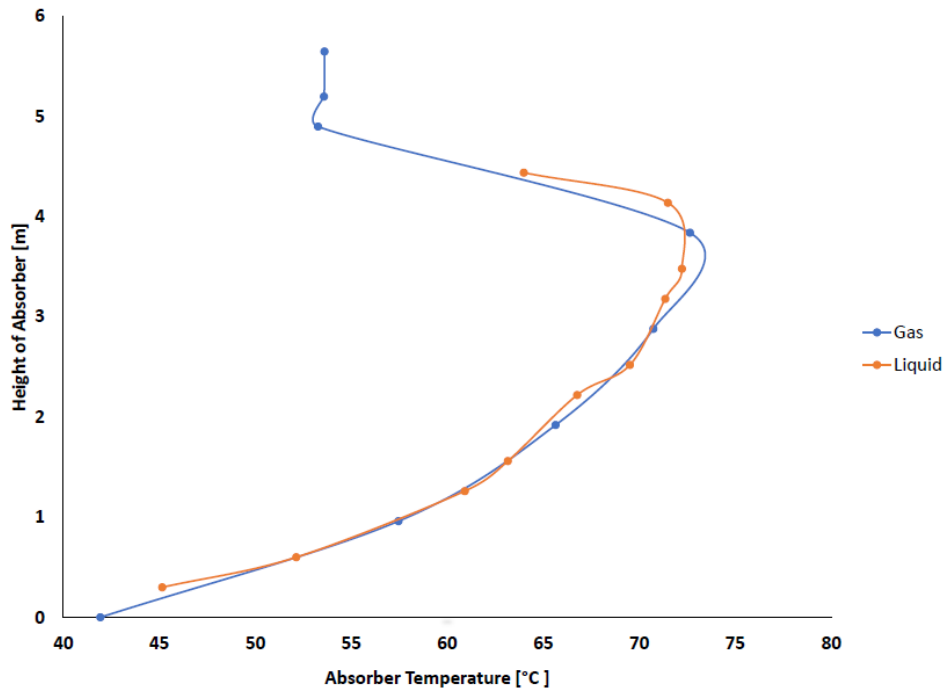

Fig. 7. Temperature profile of the absorber for benchmark test. The blue line represents gas temperature and orange line represents the liquid side temperature inside of the absorber column. The vertical axis represents the height of the column in meters.
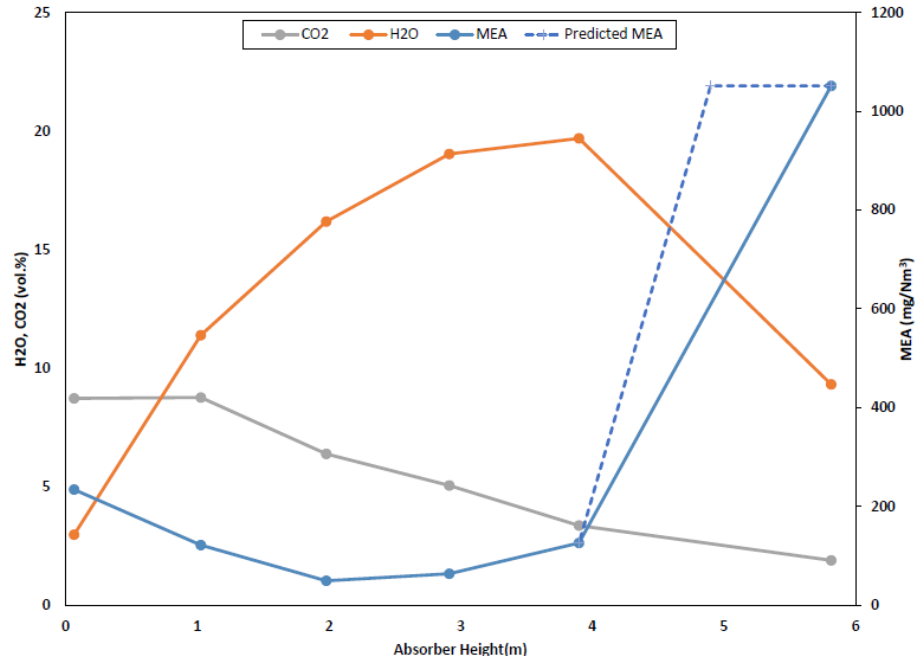
Fig. 8. FTIR measurements of water and CO_2 content in vol. % along with MEA content (mg/Nm³) along the absorber column for the benchmark test. MEA content first decreases until 2m and then starts increasing gradually. Between the maximum temperature point in the column (3.9m) until the exit of the column, MEA content increases from 125mg/Nm³ to 1051 mg/Nm³
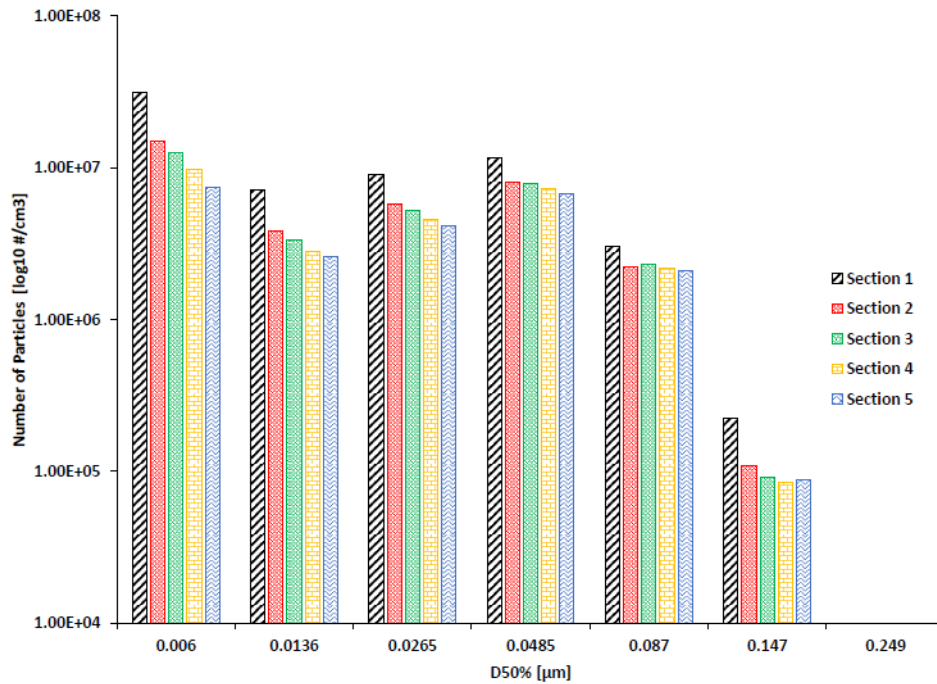

Fig. 9. Particle size distribution of the benchmark test. The different colours of bar represent the measurement at different position of the absorber column, with Section 1 representing the inlet and section 5 as the top most section of the absorber column. The graph represents the particle concentration averaged over a duration of 5 minutes. The relative standard deviation was calculated to be within 6%
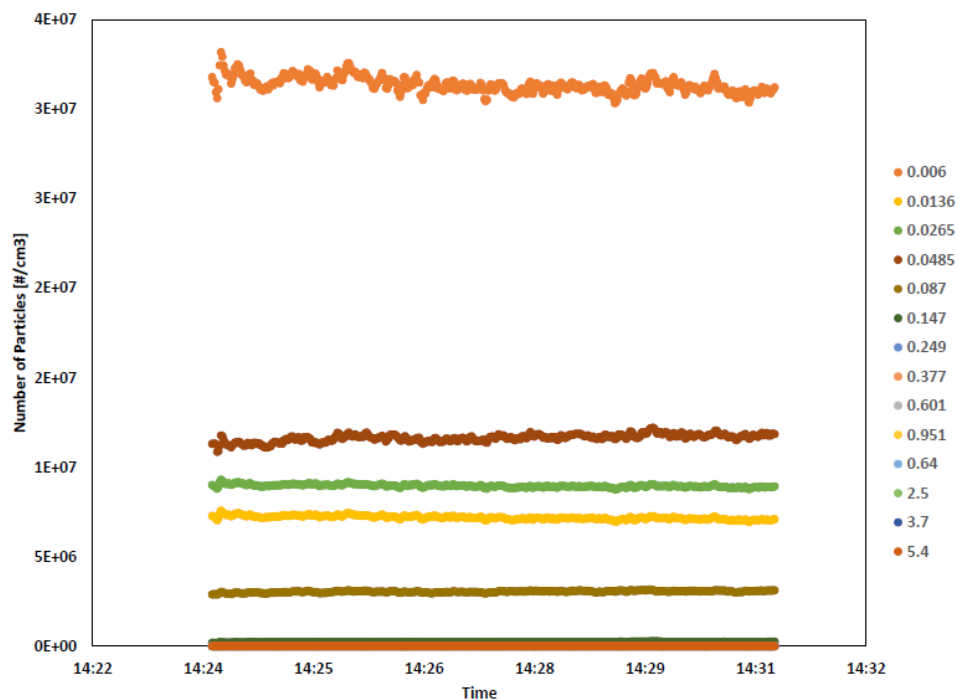
Fig. 10. Particle size distribution as measured by ELPI+ at the inlet section of absorber column for the benchmark test. Particle size mentioned are in microns. This figure is intended to show the stability of the measured value by ELPI+. The standard deviation of total particle concentration (sum of particle concentration across all size range) was found to be $6.42 \times 10^5/cm^3$ and has a relative standard deviation of 1%.

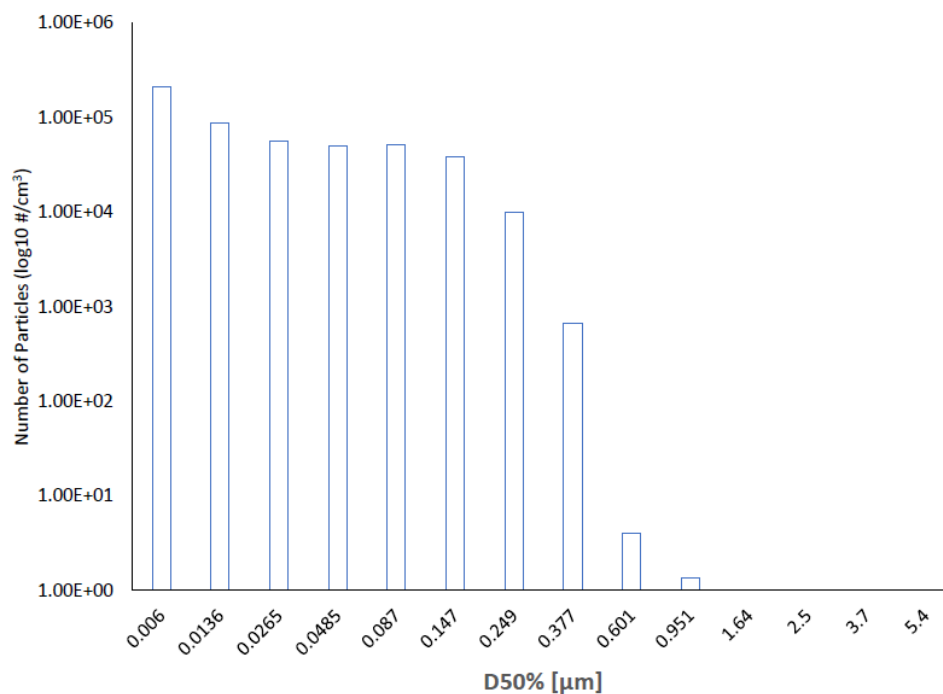Fig. 11. Particle size distribution of outside air. Large size particles of upto 0.951μm were measured, while inside the column the largest particles measured was 0.147 μm.

2.6.4.2. Particle number concentration and size distribution

Before the start of the particle size measurement at various locations of the absorber, it was made sure that the mini-plant was operating at stable conditions for at least one hour. The stability of the measurements can be seen in Fig.10. Particle size distribution (after incorporating the dilution factor) at various gas sampling positions were as shown in Fig 9. Aerosols were recorded for a period of 5-6 minutes, and particle concentrations and respective mass were calculated as an average over the duration of measurement. Maximum Relative Standard Deviation (RSD) for these measurements was found to be 6% from the averaged value. Experiments with and without aerosol causing nuclei (section 2.6.5) were performed on the same day to avoid any influence of external factors. On the other hand, tests which involved use of empty column (section 2.6.3 and 2.6.6) were performed on subsequent days.

From Fig.9 it is observed that for the benchmark test, on an average 6.24×10^7 #/cm^3 particles are measured at the inlet, while at the exit of column (section 5) 63.1% of the particles are lost, resulting in a total number concentration of 2.3×10^7 #/cm^3 In terms of the particle size distribution, particles from 0.006-0.147μm are recorded, with a majority in the smallest stage. Particle measurement of outside air were also made to observe the particle size distribution as seen in Fig.11. From the figure it is observed that particles as large as 0.951μm are observed, thereby eliminating the possibility of ELPI+ measurement error.

Table 6. Overview of results of the benchmark test. The number of particles at inlet (section 1) and exit (section 5) are represented as the average of the duration of measurement. Standard deviation for the inlet particle measurements was 6.42×10^5 and at exit (section 5) was 2.93×10^5. Refer to Fig.1 for exact location of particles measurement.

Number of particles at Inlet (Section 1) [#/cm^3]	Number of particles at exit (Section 5) of absorber [#/cm^3]	Absorber outlet CO_2 content [vol%]	CO_2 capture rate [%]
6.24×10^7	2.3×10^7	1.9	87

2.6.4.3. Aerosol Behavior

Based on the particle measurements performed for the benchmark test, some analyses were performed to better understand the behavior of aerosols along the column. From Table.9, an overall decrease in the particle number concentration is observed. This decrease in particle number concentration may result from agglomeration or particles hitting on solid surfaces or both.

Table 7. Total particle concentration and corresponding total mass of particles across the column.

Column Height (m)	Total Number of particles (#/cm^3)	Total mass of particles (mg/Nm^3)
3.9	2.30×10^7	1.32
2.91	2.60×10^7	1.37
1.98	3.15×10^7	1.48
1.02	3.50×10^7	1.50
0.06	6.24×10^7	2.22

Table 7 represents the difference in the number of particles between two consecutive sections in the column which is referred to as ΔN. A negative value of ΔN indicates that the number concentration is lower at the higher of the two stages. From Table.7, an increase in particle number concentration for 0.147μm between section 4-5 is observed – indicating a PSD shift to right. This shift towards right along with decreasing particle number concentration indicates that the governing mechanism is agglomeration of particles as seen in Table.3. Also, from

Table.9, decrease in mass concentration across the column is observed – which along with decreasing particle number concentration attributes to hitting on solid surfaces.

Table.8. Calculation of difference in the number of particles between two consecutive sections of the column for all the measured size fraction in the case of the benchmark test. For example, ΔN (1-2) represents the difference in number of particles at section 2 and section 1

D50% (μm)	0.006	0.0136	0.0265	0.0485	0.087	0.147
ΔN (4-5) [#/cm^3]	-2.31x10^6	-2.53x10^5	-3.58x10^5	-5.70x10^5	-6.62x10^4	2.59x10^3
ΔN (3-4) [#/cm^3]	-2.81x10^6	-5.19x10^5	-7.56x10^5	-6.43x10^5	-1.39x10^5	-7.75x10^3
ΔN (2-3) [#/cm^3]	-2.46x10^6	-4.96x10^5	-4.57x10^5	-1.55x10^5	7.45x10^4	-1.76x10^4
ΔN (1-2) [#/cm^3]	-1.64x10^7	-3.34x10^6	-3.21x10^6	-3.53x10^6	-8.07x10^5	-1.14x10^5

Table.9 represents values of ΔN_{total}% (ratio of "difference in total particle concentration between two consecutive sections" to "total particle concentration at the lower section"). Also, it is observed that the value of $\Delta N_{total,1-2}$% (between section 1 and 2) were significantly higher than the ΔN_{total}% at subsequent sections. The high $\Delta N_{total,1-2}$% can be accounted to the fact that the gas stream changes direction at the inlet of the column as discussed earlier. The flue gas enters the column through a horizontal heated line of 0.95cm diameter. Upon entering the column, the gas starts flowing vertically up the column which has a diameter of 4.5cm. This sudden change in orientation in flow of gas along with the change in cross sectional area results in higher impaction of aerosols with surfaces and thereby loss of particles. The slight variation in ΔN_{total}% for rest of the section would be a result of the varying hydrodynamics occurring within the column. Table 9. indicates the total particles concentration and total mass of aerosols along the column.

The effect of agglomeration of aerosol molecules can be observed from Fig.12. The figure shows the percent of particles at a size fraction across the column, as a function of total particle concentration at the corresponding location of the column. For example, particles concentration at inlet for 0.0485μm is 18.6% of the total particle concentration at inlet, while at 3.9m the contribution of 0.0485μm is 29.2% From Fig.12 it is observed that for 0.006μm, the inlet particle concentration is ca.50% of total particles at inlet and it reduces to 32% of total particles concentration at a column height of 3.9m. There is no significant change in contribution of 0.0136μm along the column. On the other hand, for particles larger than 0.0136μm, the percentage contribution increases from inlet to 3.9m.

Comparing vapour based MEA emissions with that of MEA emissions during benchmark test, it is noted that 670mg/Nm3 (Total Emission =1051 – Vapour emission=381) of MEA emissions are caused due to aerosols. Assuming a 5mol/L MEA concentration in the aerosol, the overall mass of aerosols can be calculated. Upon calculation, it is found that a combined aerosol mass of 2.2g/Nm3 is needed to account for 670mg/Nm3 of MEA. However, at a height of 3.9m, the aerosols account to only 1.32mg/Nm3 in mass instead of the required 2.2g/Nm3. This is an indication that a large proportion of bigger particles are not being observed. To further validate the theory, it is assumed that 105 more particles exist at section 5 of the column in such a way that these particles are equally distributed in all the size fractions between 0.249μm and 5.4μm. An addition of 10000 particles, increases the total particle concentration to 2.31x10^7/cm^3. For this new particle size distribution, the total mass of particle was calculated and found to be 1.2g/Nm3. This signifies that even an addition of 10000 particles per stage between 0.249 and 5.4μm would not account to the required total aerosol mass of 2.2g/Nm3. This observation further justifies that a fraction (greater than 10000 particles) of large particles are not being observed by ELPI+ inside the column for benchmark test.

Table 9. Data representing the value of $\Delta N_{total}\%$ between two consecutive sections in the column

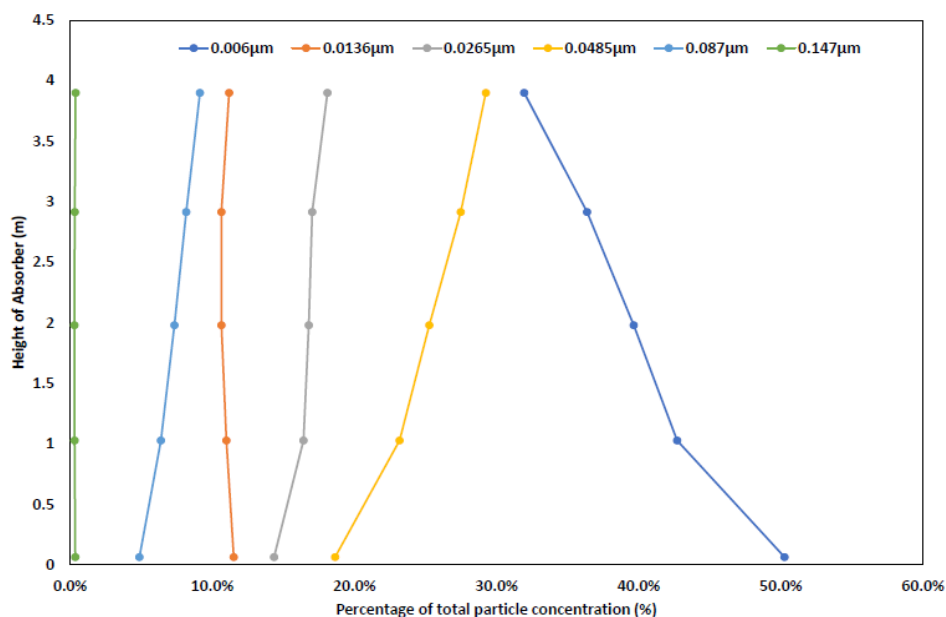| Test Conditions/ $\Delta N_{total}\%$	$\Delta N_{total,1-2}\%$	$\Delta N_{total,2-3}\%$	$\Delta N_{total,3-4}\%$	$\Delta N_{total,4-5}\%$
With SO$_2$	-44	-10	-15	-13
Without SO$_2$	-40	-14	-12	-9

Fig. 12. Particle concentration at every size fraction across the column as a function of the total particle concentration at the corresponding section in the column. It is observed that the contribution of 0.006μm reduces from 50% to 32% along the column, while the contribution of 0.0265μm, 0.0485μm and 0.087μm increases along the column

2.6.5. Effect SO$_2$ in Flue gas

To better understand the contribution of aerosols to the total emission a test was performed without the presence of SO$_2$ in the flue gas stream. For this, the SO$_2$ stream through the catalytic fixed bed reactor was switched off, while other gases passed through it. All other parameters were set at the same values as in the benchmark test. Table 10. shows the operating conditions of the pilot plant in the absence of SO$_2$ in flue gas.

Based on the measured value of amine exiting the absorber as shown in Fig.16, it can be observed that there is a drastic decrease in MEA emissions. In the benchmark test with SO$_2$ in the flue gas, MEA emission was recorded as ca. 1051mg/Nm^3, while in the absence of SO$_2$, MEA emissions were recorded was ca. 381 mg/Nm^3. Capture rate of CO$_2$ in both the scenarios were comparable with 87% and 84% respectively. To ensure that the condition between the two tests were similar, the CO$_2$ content in the lean solvent were maintained at 1.41mol CO$_2$/L MEA and 1.46 mol CO$_2$/L MEA, respectively.

Table 10. Operating condition of Capture plant for the test in the absence of SO2 in flue gas

Gas Flow (m^3)	Solvent Flow (kg/h)	Inlet solvent temperature (°C)	Inlet gas temperature (°C)	CO_2 content at Inlet (vol %)	Stripper Pressure (mbar)	CO_2 content - lean solvent (mol CO_2/L MEA)
4.17	20±0.08	43.5±0.1	44.4±0.6	12.5	871.7±4.22	1.46

Table 11. Overview of results in the absence of SO2 in the flue gas compared with to SO2 being present in the flue gas

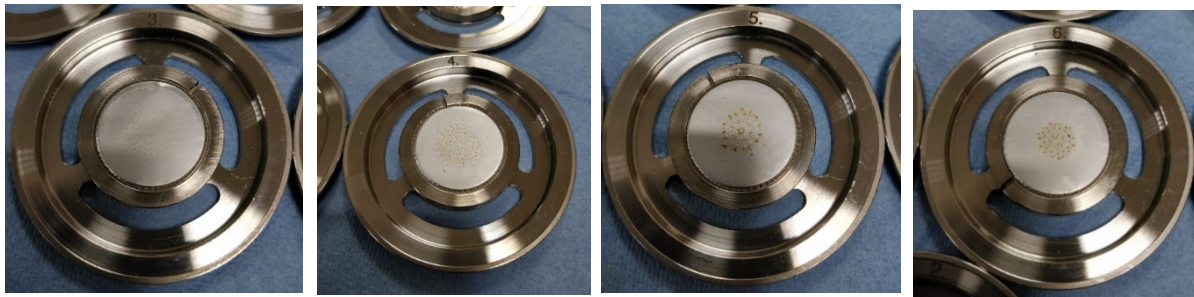| Test	Number of particles at Inlet (#/cm^3)	Number of particles at top of absorber (#/cm^3)	Absorber outlet CO_2 content (vol%)	Absorber Outlet MEA content (mg/Nm^3)	CO_2 capture rate (%)
Without SO_2	$2.71x10^7$	$1.12x10^7$	2.1	383±12.6	84
With SO_2	$6.24x10^7$	$2.30x10^7$	1.63	1051±15.6	87

Fig. 13. Images of greased aluminium foils used in the ELPI+ during this study. The foils on the impactor were not changed during the study. From top left: Stage 3 (0.0265μm), Stage 4(0.0485μm), Stage 5 (0.087μm) and Stage 6 (0.147μm) on the bottom.

It is observed that even in the absence of SO_2 in the flue gas, there are many particles and/or aerosols that are entering the absorption column. This is possibly due to the fines of the catalyst that are present inside of the fixed bed reactor. Difference in number of particles at the inlet of the column with and without SO_2 in the flue gas would give a good estimation of aerosols purely due to H_2SO_4 droplets in the flue gas. This estimation of particles size distribution is shown in Table.12 and is referred to as "δ".

Fig.14 compares the particle and mass concentration by each size fraction to total particle and mass concentration at inlet of absorber column in the presence and absence of SO_2 in flue gas. The plot enables us to compare the particle and mass distribution across the different size fractions when aerosol causing nuclei are present and absent in the flue gas. It has to be noted that for the size fraction of 0.147μm the particle and mass contribution in case of "No SO_2 in FG" is zero, indicating that particles at this size fraction do no exist in the absence of SO_2 in flue gas. Moreover, for the size range of 0.0487μm, 0.087μm and 0.147μm, there is a significant increase in particle contribution in the presence of SO_2 in flue gas. Linking the increase in number of particles formed due to the presence of H_2SO_4 particles with increased MEA emissions at the exit of absorber, it is concluded sulphuric acid aerosols of the size fraction of 0.0485μm-0.147μm are the aerosol nuclei for MEA emissions. This observation can further be verified by at the greased foils in the ELPI+ as shown in Fig.13. On the foils of stages 4 (0.0485μm),5 (0.087μm) and 6 (0.147 μm), yellow spots are observed while that on Stage 3 are missing. These are interpreted as an indication of the presence of MEA, which is carried away with aerosols predominantly in the size 0.0485μm – 0.147μm fraction.

Table 12. Size distribution of aerosols entering the absorber both in the presence and absence of SO2 in the flue gas. The difference of the two. (represented as "δ") would represent an estimation of aerosols purely caused by the presence of SO2 in the flue gas

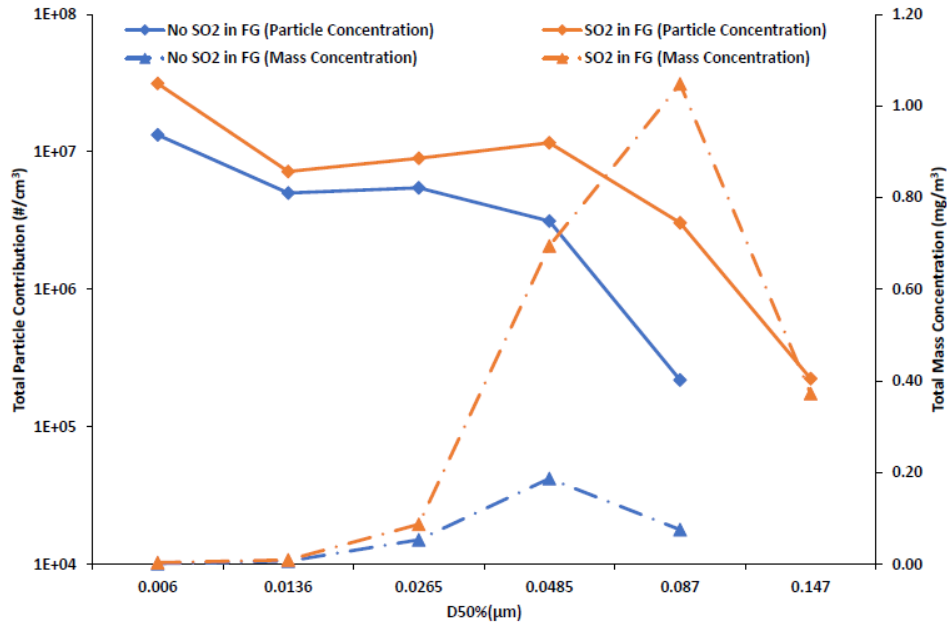| D50%(µm)		0.006	0.0136	0.0265	0.0485	0.087	0.147
Number of Particles (#/cm³)	With SO$_2$	3.14×10^7	7.18×10^6	8.95×10^6	1.16×10^7	3.04×10^6	2.24×10^5
	Without SO2	1.33×10^7	5.01×10^6	5.47×10^6	3.13×10^6	2.19×10^5	0.0
	δ	1.81×10^7	2.18×10^6	3.48×10^6	8.50×10^6	2.82×10^6	2.24×10^5

.

Fig. 14. Plot comparing particle (blue) and mass (orange) concentration by each size fraction to total particle (solid line) and mass (broken line) concentration in the presence and absence of aerosol causing SO$_2$ molecules in flue gas at the inlet of the absorber column. It can be noted that for size range of 0.0485µm-0.147 µm, there is an increase in mass concentration in the presence of SO$_2$ in flue gas and particles of 0.147 µm do not exist in the absence of SO$_2$ in flue gas.

Also, similar to that observed in the benchmark test, agglomeration of particles was based. This can be seen from Fig.15, where percentage contribution by 0.006µm and 0.0136 µm decreases across the column, and increases for 0.0265µm, 0.0485µm and 0.087µm.
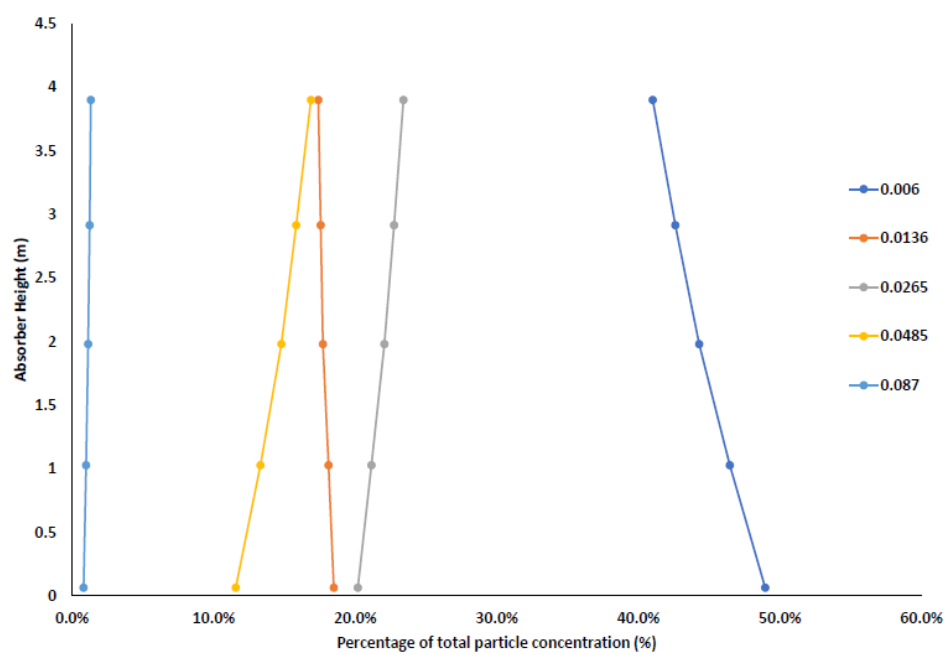
Fig. 15. Particle concentration at every size fraction as a function of total particle concentration at the corresponding section in the column in the case of flue gas without SO_2
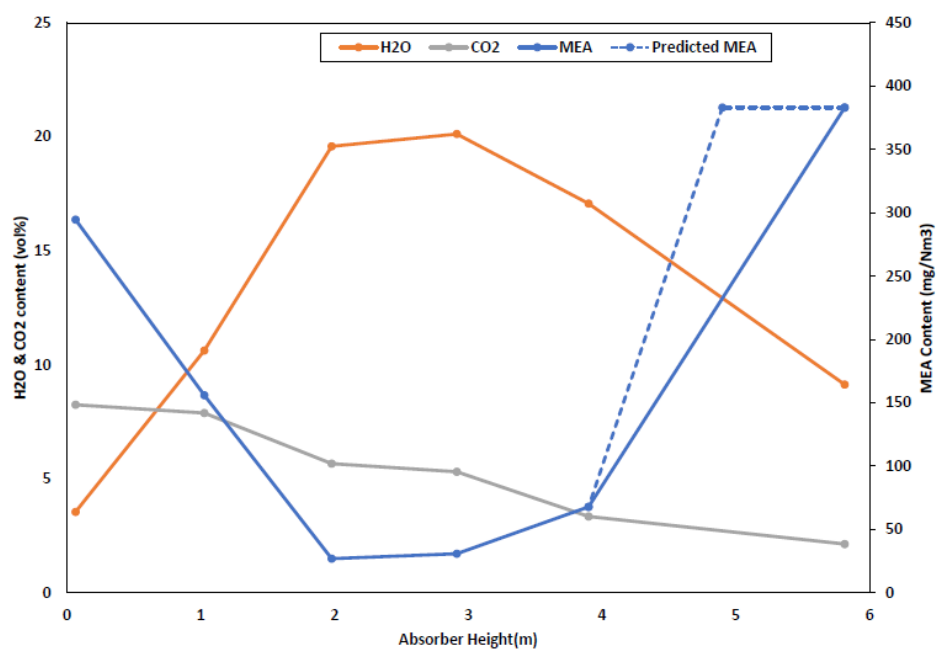

Fig. 16. Plot representing MEA (mg/Nm³), CO_2 (vol.%) and water (vol.%) in gas phase across the column as measured by FTIR in the absence of SO_2 in the flue gas.

2.6.6. Effect of Dilution System

Diluting the gas sample can have a significant impact on the particle size distribution [19]. The water in the particle tends to evaporate due to the use of dry dilution air and at a higher temperature than the sample flue gas. The effect is limited to a point wherein the droplets have reached the "dry droplet diameter" wherein no further water can evaporate due to an extremely high local vapor pressure.

Measurement of aerosols without the use of the diluter system for the benchmark test were not possible due to the high moisture content, which could damage the corona charger inside of the ELPI+. In order to understand the effect of dilution, tests without the diluter system were performed in the empty column mode (absence of solvent flow).

Fig.17. shows the particle size distribution measured along the column in the absence of a dilution system under empty column settings. This PSD could be compared with Fig.5 (with Diluter in empty column setting) and observed that the distribution is quite similar. Also, the total particle concentration in the absence of dilution system ranges from 2.48×10^7- 5.67×10^7 /cm^3, which is similar to that observed in the presence of diluter where the particle concentration ranged from 2.06×10^7 – 4.74×10^7/cm^3. Although the total particle number concentration recorded is high (order of magnitude 10^7/cm^3), the total mass of these particles is still in the range of few mg/m^3.

To compare the distribution directly with and without diluter, the distribution is plotted (Fig.18) for Section 2 (1.025m) and Section 3 (1.985m) of the absorber. From the figure it is observed that the distribution in the presence and absence of dilution system is very similar. Moreover, in either case of dilution system being present or absent, particles larger than 0.147μm are not observed. This eliminates the possibility of dilution system having a significant effect on the distribution of particles and causing them to shrink.
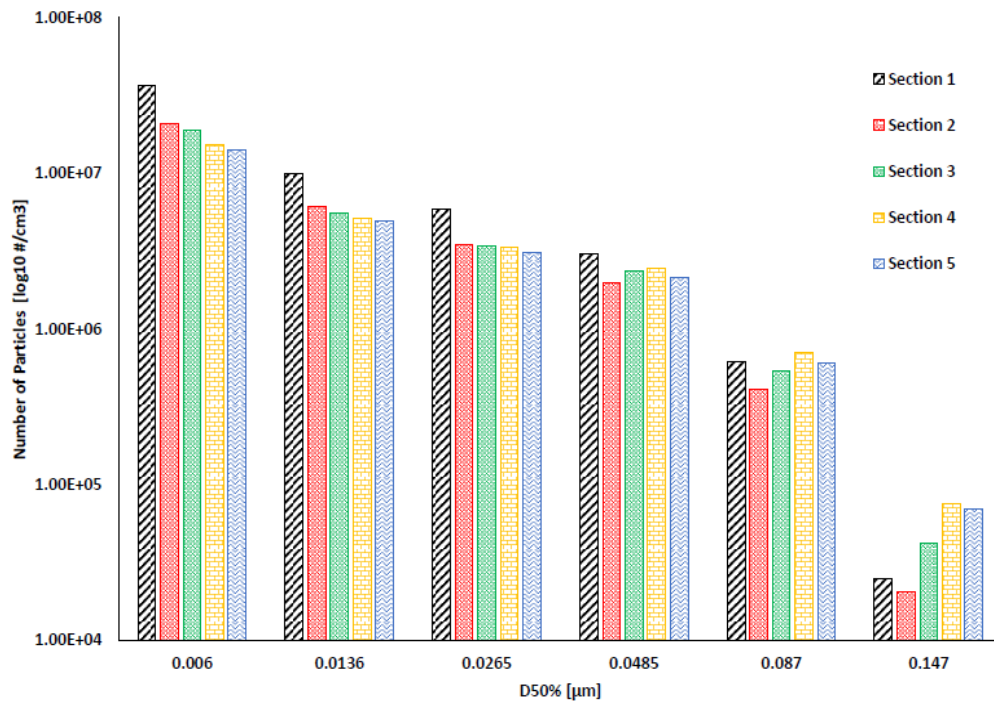

Fig. 17. Particle size distribution in the absence of Dilution System in Empty Column mode. It is observed that particles larger than 0.147μm were not observed.
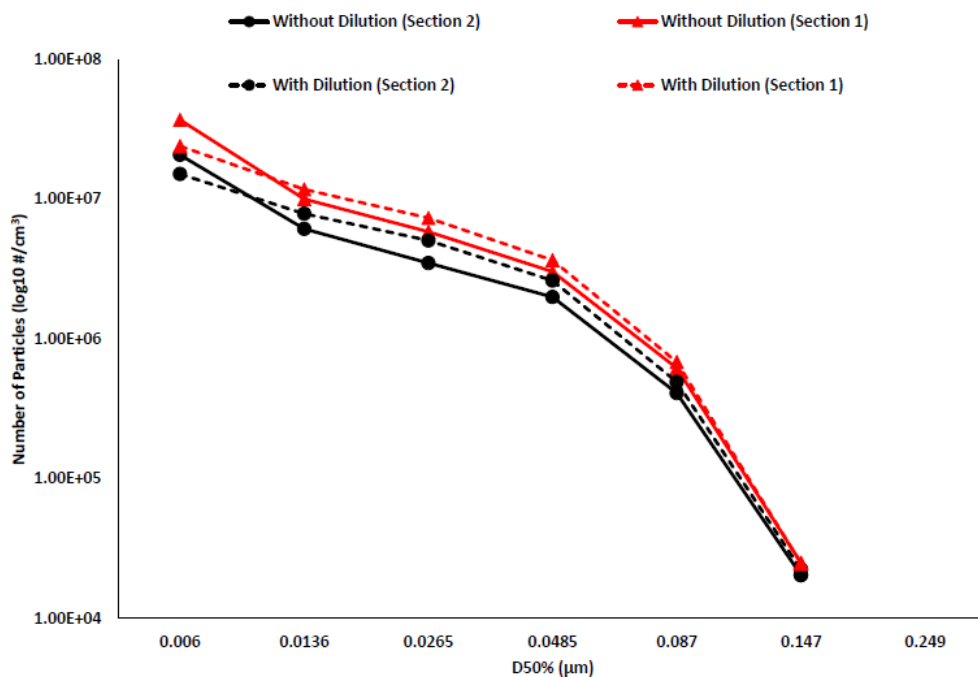
Fig. 18. Comparison of particle size distribution with (dotted) and without (solid) dilution system in empty column mode. For comparison, distribution at Section 2 (black) and Section 3 (Red) is plotted. It is seen that the distribution in the presence and absence of dilution system is not heavily affected. Moreover, particles larger than 0.147µm is not observed in either cases.

3. Conclusion

This study was conducted to understand the mechanism of aerosols across the absorber column in a post combustion carbon capture plant. The experimental study was performed in a bench scale CO_2 capture plant at TNO, Delft. Particles entering the column (in the presence of SO_2 in the flue gas) exceeded $10^7 cm^{-3}$ in concentration. The corresponding amine emissions were recorded as 1051mg/Nm^3. Up until the temperature bulge in the column, MEA content was within the vapour emission range. Upon crossing the temperature bulge, when the temperature reduces in the top 1/3rd of the column, amine in the vapour phase condenses on to the aerosol phase rather than the bulk liquid phase, resulting in the drastic increase in MEA content. Total particles concentration at the inlet in the absence of SO_2 in the flue gas reduced by over 50% and were less than 0.087µm in size. The amine emissions were recorded to be 381mg/Nm^3. The results indicate that agglomeration of particles to form larger particles occurred, with percentage contribution of 0.006µm and 0.0136µm to total particle concentration decreasing from 50% and 11.5% at inlet to 32% and 11.2% at exit, while particles in size fraction range 0.0265µm – 0.147µm increased from inlet to exit for the benchmark test. The increase in size of particles across the column along with sudden increase in MEA emissions at the top of the column indicates that while aerosols grow "gradually" by means of agglomeration along the column, MEA emission only increases at the top of the column beyond the point of temperature bulge. A decrease of overall particle concentration ($6.24 \times 10^7/cm^3$ at inlet to $2.30 \times 10^7/cm^3$ at exit) and aerosol mass (2.22mg/m^3 at inlet to 1.32mg/m^3 at exit) along the column indicated that along with agglomeration of particles, loss of mass and particles due to hitting of aerosols on the solid surfaces was also observed. The mismatch of mass of aerosol and MEA (1.32mg/m^3 of aerosol mass and MEA of 125.8mg/m^3) at section 5 was a clear indication of incomplete measurement of particle size distribution. However, the total particle concentration of $\sim 10^7/cm^3$ and its corresponding MEA content at the exit ($\sim$1000mg/Nm^3) are in good agreement when compared to literature. The absence of dilution system did not give rise to particles larger than 0.147µm and thereby eliminating the possibility of dilution system causing the underestimation of aerosols size. The reason for not observing larger particles cannot be explained at this moment and requires further investigation.

As a follow up work, tests looking at the impact of operating conditions on the trend and extent of MEA increase along the absorber column will be performed. Additional particle measurement devices which can capture the larger particles to account for the total mass will be added to the test equipment to get a complete overview of the particle size and mass distribution.

References

[1] Climate change 2007: "Mitigation of climate change contribution of Working Group III to the fourth assessment Report of the Intergovernmental panel on Climate Change." *Intergovernmental Panel on Climate Change -2007,* 45(09)

[2] NOAA.(2017,March).Carbon dioxide levels rose at record pace for 2nd straight year. Retrieved from http://www.noaa.gov/news/carbon-dioxide-levels-rose-at-record-pace-for-2nd-straight-year

[3] MIT. The Future of Coal-Options for a Carbon Constrained World. 2007.

[4] T. Kamijo *et al.*, "SO3 Impact on Amine Emission and Emission Reduction Technology," *Energy Procedia*, vol. 37, pp. 1793–1796, 2013

[5] De Koeijer,G., Enge, Y.,Sanden,K.,Graff,O.F.,Falk-Pedersen,O.,Amundesen,T.,Overa,S.,"CO₂ Technology Center Mongstad-design, functionality and emissions of amine plant" , *Energy Proc.*4,1207-1213,2011

[6] I. Sreedhar, Tanisha Nahar, A. Venugopal, B. Srinivas, "Carbon capture by absorption – Path covered and ahead", *Renewable and Sustainable Energy Reviews*, Vol. 76, pp.1080-1107, 2017.

[7] P. Khakharia *et al.*, "Investigation of aerosol based emission of MEA due to sulphuric acid aerosol and soot in a Post Combustion CO2 Capture process," *Int. J. Greenh. Gas Control*, vol. 19, pp. 138–144, Nov. 2013

[8] Jr. Pitts J.N., D. Grosjean, K.V. Cauwenberghe, J.P. Schmid, and D.R. Fitz. "Photooxidation of Aliphatic Amines Under Simulated atmospheric Conditions: Formation of Nitrosamines, Nitramines, Amides, and Photochemical Oxidant". In: *Environmental Science and Technology* 12.8 (1978), pp. 946–953.

[9] A.R. Tricker and R. Preussmann. "Carcinogenic N-nitrosamines in the diet: occurrence, formation, mechanisms and carcinogenic potential". In:*Mutation Research/Genetic Toxicology* 259.3 (1991), pp. 277– 289.

[10] P. Khakharia, H. M. Kvamsdal, E. F. da Silva, T. J. H. Vlugt, E. Goetheer, and E. F. da Silva, "Field study of a Brownian Demister Unit to reduce aerosol based emission from a Post Combustion CO2 Capture plant," *Int. J. Greenh. Gas Control*, vol. 28, pp. 57–64, Sep. 2014

[11] R. K. Srivastava, C. A. Miller, C. Erickson, and R. Jambhekar, "Emissions of Sulfur Trioxide from Coal-Fired Power Plants," *J. Air Waste Manage. Assoc.*, vol. 54, no. 6, pp. 750–762, Aug. 2004.

[12] Mimura, T.; Nojo, T.; Ishida, K.; Nakashoji, H.; Tanaka, H.; Hirata, T., "Amine Recovery Method and Apparatus and Decaronation Apparatus having same", *US 6,784,320 B2* Aug. 31, 2004.

[13] H. Majeed, H. Knuutila, M. Hillestad, and H. F. Svendsen, "Gas phase amine depletion created by aerosol formation and growth," *Int. J. Greenh. Gas Control*, vol. 64, pp. 212–222, Sep. 2017

[14] Jia-Lin Kang, Yue Zhang, Steven Fulk, and Gary T.Rochelle, "Modeling Amine Aerosol Growth in the Absorber and Water Wash," *Energy Procedia*, vol. 114, pp. 959–976, Jul. 2017.

[15] P. Khakharia *et al.*, "Understanding aerosol based emissions in a Post Combustion CO2 Capture process: Parameter testing and mechanisms," *Int. J. Greenh. Gas Control*, vol. 34, pp. 63–74, Mar. 2015

[16] Hammad Majeed, Hallvard F. Svendsen, "Characterization of aerosol emissions from CO2 capture plants treating various power plant and industrial flue gases", *International Journal of Greenhouse Gas Control*, Vol 74, pp. 282-295, 2018.

[17] Hammad Majeed, Hanna K. Knuutila, Magne Hillestad, Hallvard F. Svendsen, "Characterization and modelling of aerosol droplet in absorption columns", *International Journal of Greenhouse Gas Control*, Vol 58, pp. 114-126,2017

[18] Yue Zhang, Jia-Lin Kanga, Steven Fulk, and Gary Rochelle, "Modeling Amine Aerosol Growth at Realistic Pilot Plant Conditions," *Energy Procedia*, vol. 114, pp. 1045–1060, Jul. 2017.

[19] Jan Mertens, L. Brachert, D. Desagher, M.L. Thielens, P. Khakharia, E. Goetheer, K. Schaber, "ELPI+ measurements of aerosol growth in an amine absorption column", *International Journal of Greenhouse Gas Control*, Vol. 23, pp. 44-50, 2014

[20] Jan Mertens, P. Khakharia, Pieter Rogiers, J. Blondeau, H. Lepaumier, E. Goetheer, B. Schallert, K. Schaber, I. Moretti, "Prevention of Mist Formation in Amine Based Carbon Capture: Field Testing Using a Wet ElectroStatic Precipitator (WESP) and a Gas-Gas Heater (GGH)", *Energy Procedia*, Vol. 114, pp. 987-999, 2017

[21] Lombardo, G., Fostås, B. F., Shah, M. I., Morken, A. K., Hvidsten, O. A., Mertens, J., & Hamborg, E. S. "Results from Aerosol Measurement in Amine Plant Treating Gas Turbine and Residue Fluidized Catalytic Cracker Flue Gases at the CO2 Technology Centre Mongstad". *Energy Procedia*, vol.114, pp. 1210–1230, 2017

[22] Saha, C., & Irvin, J. H. "Real-time aerosol measurements in pilot scale coal fired post-combustion CO₂ capture". *Journal of Aerosol Science,* vol *104*, pp43–57, 2017.

[23] Peter Moser, Georg Wiechers, Knut Stahl, Torsten Stoffregen, Gerald Vorberg, Gustavo A. Lozano, "Solid Particles as Nuclei for Aerosol Formation and Cause of Emissions – Results from the Post-combustion Capture Pilot Plant at Niederaussem", *Energy Procedia*, Vol.114, pp.1000-1016, 2017.

[24] L. Brachert , T. Kochenburger & K. Schaber, "Facing the Sulfuric Acid Aerosol Problem in Flue Gas Cleaning: Pilot Plant Experiments and Simulation", *Aerosol Science and Technology*, Vol.47, pp. 1083-1091, 2013

[25] Krepff, Robert. Conversion of SO₂ to SO₃ with a catalyst of selected porosity, US3275406A, United States Patent and Trademark Office, 27 September 1966

[26] Steven M. Fulk, Gary T. Rochelle, "Quantification of Gas and Aerosol-phase Piperazine Emissions by FTIR Under Variable Bench-scale Absorber Conditions", *Energy Procedia*, Vol. 63,pp. 871-883, 2014

[27]A. Järvinen, M. Aitomaa, A. Rostedt, J. Keskinen, J. Yli-Ojanperä, "Calibration of the new electrical low pressure impactor(ELPI+)", *Journal of Aerosol Science*, vol. 69, pp.150-159,2014.

[28] Mohammad R.M. Abu-Zahra, Léon H.J. Schneiders, John P.M. Niederer, Paul H.M. Feron, Geert F. Versteeg, "CO2 capture from power plants: Part I. A parametric study of the technical performance based on monoethanolamine", *International Journal of Greenhouse Gas Control,*Volume vol 1,pp. 37-46, 2007

[29] P. Moser, S. Schmidt, G. Sieder, H. Garcia, and T. Stoffregen, "Performance of mea in a long-term test at the post-combustion capture pilot plant in niederaussem", *International Journal of Greenhouse Gas Control,* Vol 5, 620, 2011

[30] Ralf Notz, Hari Prasad Mangalapally, Hans Hasse, "Post combustion CO2 capture by reactive absorption: Pilot plant description and results of systematic studies with MEA", *International Journal of Greenhouse Gas Control*, Vol 6, pp.84-112,2012.